

# QUANTITATIVE DETERMINATION OF SEGREGATION EFFECTS FOR ADN-BASED LIQUID MONOPROPELLANTS DUE TO INTERNAL FLOW PHENOMENA

Christian Hendrich<sup>(1)</sup>, Philipp Müller<sup>(1)</sup>, Marius Wilhelm<sup>(1)</sup>, Matthias Haßler<sup>(2)</sup>, Stefan Schleichriem<sup>(1)</sup>

<sup>(1)</sup> Institute of Space Propulsion, German Aerospace Center (DLR), 74239 Hardthausen, Germany,  
Email: Christian.Hendrich@dlr.de

<sup>(2)</sup> Technical University Munich (DLR), 80333 Munich, Germany,  
Email: Matthias.hassler@tum.de

**KEYWORDS:** ADN-based monopropellants, Cavitation, Injection, Segregation, UWS

## ABSTRACT:

For this paper the internal flow behaviour of urea-water-solutions (UWS) and possible salt segregation was investigated. The UWS is used as a simuli for ammonium dinitramide (ADN). For the investigation the optical refraction method is used. The injectors itself consist of transparent polymethylmethacrylate (PMMA). Three different concentrations on three different temperature levels were tested. However, as soon as cavitation occurs inside the injector, segregation incepts, accumulating the salt upstream.

## 1. INTRODUCTION

Ammonium dinitramide-based liquid monopropellants are currently under investigation to replace hydrazine as propellant for satellite thrusters. A trigger for developing alternatives is the complexity in handling hydrazine due to its toxicity. Additionally, hydrazine has been put on the list of substances of very high concern (SVHC) by ECHA. Two promising candidates for the replacement are FLP-106 and LMP-103S [1,2]

One of the downsides of these ADN-based monopropellants is their lack of cold-start capability. Ideally, a thermal ignition is desired since the catalyst bed needs constant heating and has the risk of poisoning before the end of life of the mission.

Before considering a thermal ignition process, parameters and boundary conditions must be well known as well as the spray morphology. Since FLP-106 and LMP-103S are multicomponent systems it is unknown how they will behave when rapidly exposed from a high pressure environment to vacuum conditions. This sudden exposure results in a so-called flash evaporation or flashing. As the environment is below the vapour pressure of the propellant and its single components, decomposition is a possible scenario with the crystallisation of the dissolved ADN-salt.

Another subject worth looking into is the internal flow field. Experiments performed by Hendrich and Schleichriem [3] showed accumulation of salt upstream of the injector after the tests. A following numerical evaluation confirmed strong cavitation over the contraction area [4]. Figure 1 shows the pressure profile over the contraction, resulting in recirculation areas inside the injector.

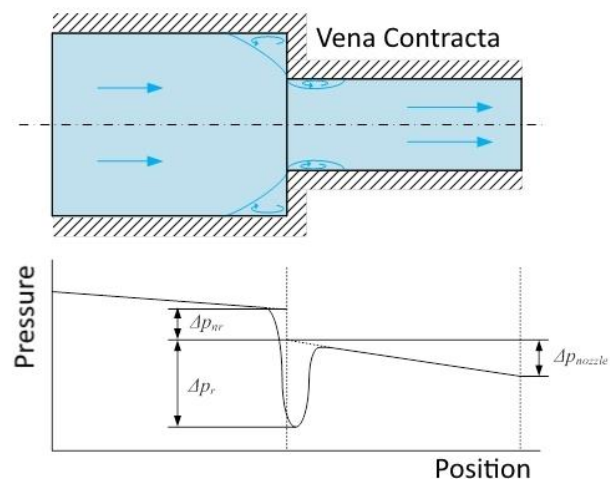


Figure 1. Top: Vena contracta and recirculation area over contraction area. Bottom: Internal pressure profile.

For ADN-based monopropellants this behaviour is potentially dangerous for missions. Occurring cavitation could lead to segregation and to clogging of crucial parts of the feed system. This already happened during tests with LMP-103S at DLR Lampoldshausen. A  $\mu$ Showerhead injector partially clogged with crystallised ADN. This is depicted in Figure 2. Clogging using LMP-103S was also already reported by Friedhoff et al. [5] and Dinardi [6].

To understand the severity of this phenomenon, a test setup was built to measure the concentration upstream of the contraction.



Figure 2: ADN-deposition after LMP-103S test; Clogged elements of  $\mu$ Showerhead injector.

## 2. MATERIALS AND SETUP

The tests were conducted with urea-water-solutions (UWS) as a simuli for ADN. Since urea and ADN are both diamines the physical properties in terms of vapour pressure, solubility and viscosity are assumed to be similar.

The injector itself is based on the geometries given by Peter et al. [7]. The injector is 50 mm in length and 1.5 mm in diameter. Resulting in a L/D-ratio of 33.3. The contraction ratio is 0.0625 with a 120° conical inlet (sharp-edged). The basic geometry is depicted in Figure 3. Further details about the injector and the test bench and can be found in [3].

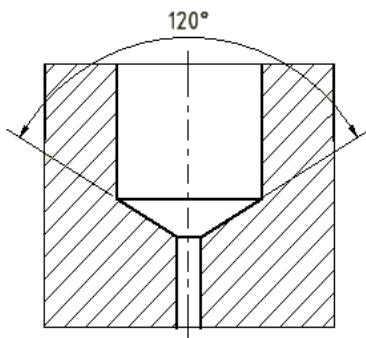


Figure 3. Inner injector geometry

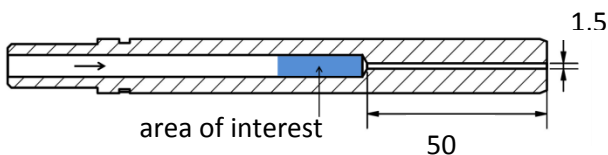


Figure 4. Injector with area of interest (blue).

To detect the degree of segregation laser refraction was used. Transparent injectors were manufactured made of polymethylmethacrylate (PMMA). Since the refractive index is a material constant it changes with changing concentration of the UWS. Therefore, it is possible to measure change if the starting concentration is known. The

refractive index is defined as relation of speed of light in vacuum to speed of light in the material.

$$n = \frac{c_{vac}}{c_{medium}} \quad \text{Eq. 1}$$

The laser beam is refracted by the injector walls when entering and exiting as well as by the fluid in the injector. The exiting beam is hitting a semi-transparent screen which is filmed and recorded during the tests. If the concentration changes during the test, the beam must also change its position on the screen. This change will be registered as "offset" to its initial position. This offset is directly proportional to the concentration. The measurement principle is depicted in Figure 5 and Figure 6.

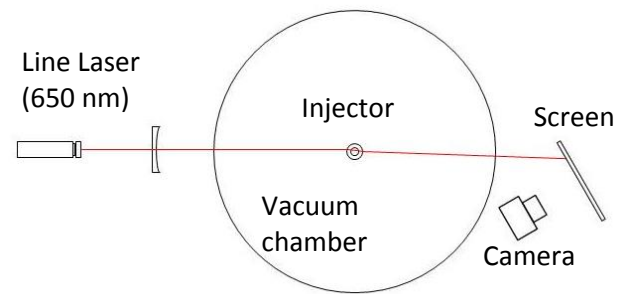


Figure 5: Measurement principle

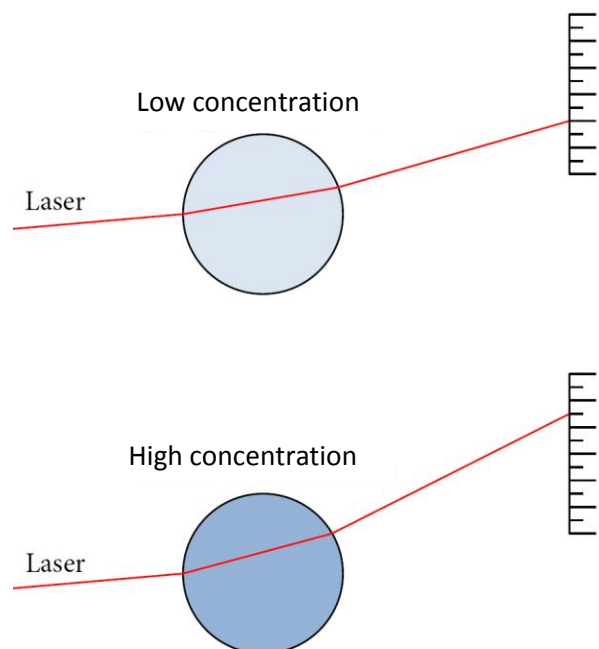


Figure 6. Top: Refraction for lower UWS concentrations. Bottom: Refraction for higher concentrated UWS.

The recorded data was analysed by a MATLAB post image processing routine. The recorded laser line was binarised leaving a white line (cp. Figure 7). In the next step the spatial information from the

semi-transparent screen was converted from mm into pixel.

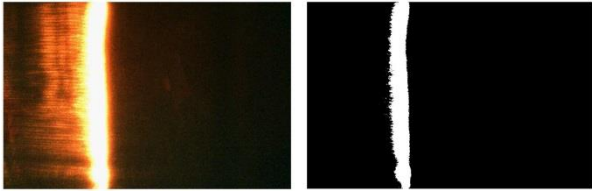


Figure 7. Left: Laser line as recorded. Right: Laser line binarised.

For all the tests a line laser (LLM-30-650) from MediaLas Electronics GmbH was used.

### 3. EXPERIMENTAL METHODOLOGY

The experiments were conducted for three temperature levels (30, 50, 70 °C) and for three concentrations (20, 30, 40 wt.-%) each. The injection pressure was kept constant at 2.7 bar. The backpressure was kept at 20 mbar. An overview over the experimental boundary conditions is given in Table 1.

Table 1. Overview of the experimental boundary conditions.

Injector L/D	33.3
Concentration [wt.-%]	20; 30; 40
$T_{inj}$ [°C]	30; 50; 70
$p_{inj}$ [bar]	2.7
$p_0$ [mbar]	20

#### 3.1 Calibration

The boundary conditions for the calibration were set that no cavitation occurs inside the injector (cf. Figure 8). Consequently, the injection pressure was set to 1.8 bar and the backpressure was ambient. The calibration was conducted with deionised water on several temperature levels as well as 20, 30 and 40 % UWS. The refractive index for water was taken from [8] and for UWS from [9]. During the calibration the laser line (baseline) was filmed from the screen; resulting in specific screen positions for every temperature and concentration. Since minor fluctuations of the laser line occur during the process, the screen position of the baseline was averaged over 2 s. Figure 9 shows the pixel offset over the internal injector position for four different water temperatures. In Figure 10 are the calibration curves for water and three UWS-concentrations depicted as function of the temperature.

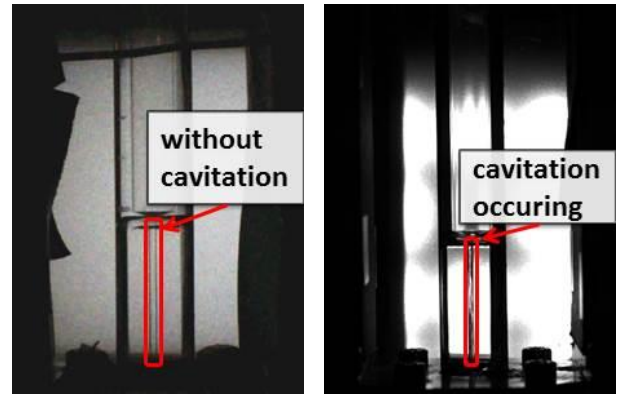


Figure 8. Internal flow. Left: Water at 50 °C and  $p_{inj} = 1.8$  bar. Right: 30 % UWS at 30 °C and 2.7 bar.

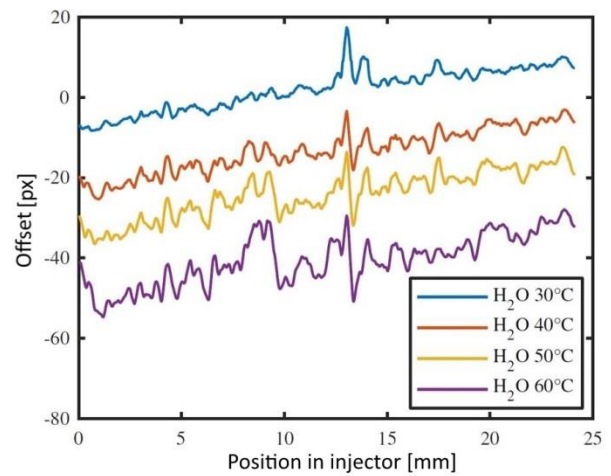


Figure 9. Pixel offset of laser line for different water temperatures.

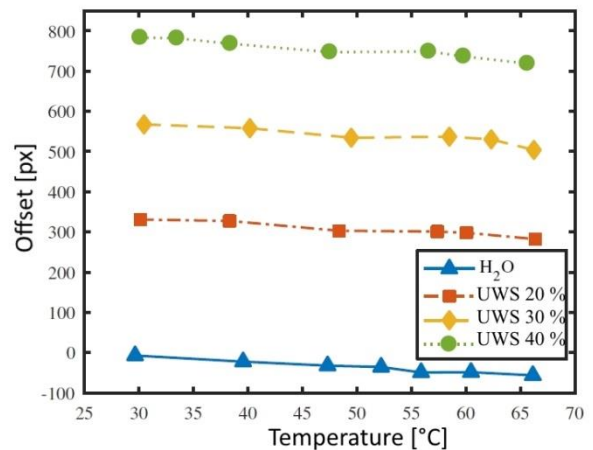


Figure 10. Calibration curves for water and different UWS-concentrations.

With the gained data it was possible to create a temperature and pixel offset-dependent function of the concentration. The surface plot follows a 2<sup>nd</sup> degree polynomial surface function and is depicted in Figure 11. The red marks indicate the measurement points.

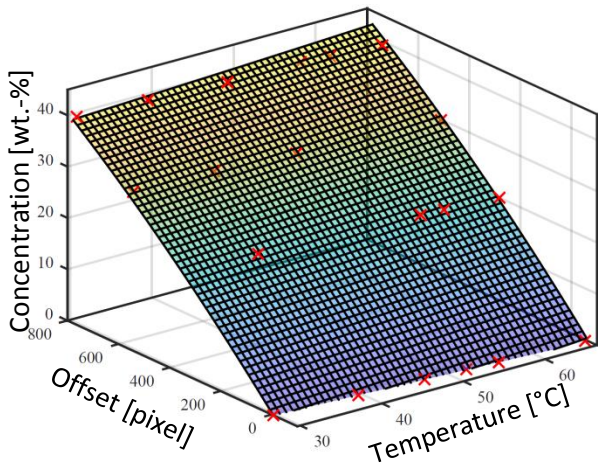


Figure 11. Function for determining the concentration in dependence of temperature and offset.

### 3.2 Test Sequence

The system was filled with the UWS and continuously circulated afterwards. During this phase the system is heated. In parallel the vacuum pumps evacuate the spray chamber. When the desired temperature is reached and homogeneously distributed, and the backpressure has reached its target value, too, the circulation pump is shut off and the system is pressurised with nitrogen. The test sequence, data acquisition and camera start.

Water with known temperature is flushed through the system for 10 s as reference for each test. This time was chosen to ensure that the flow has reached steady state. After a short pause, the 3/2-solenoid valve, separating the pressure/heating system and the vacuum chamber, opens. Injection with UWS for 55 s follows. The valve closes with additional subsequent water flushing as another reference and to flush out potential residues.

## 4. RESULTS

### 4.1 Influence of temperature

The conducted tests on three temperature levels have shown no significant influence on the degree of segregation. For all temperatures, the degree of segregation is within the measurement error margin. The change of concentration overlaps the influence of temperature respectively. This can be seen in Figure 9 and 10. Whilst the change of concentration is in increments of 200 to 300 px, the change of temperature is 70 px at most.

### 4.2 Concentration

In Figure 12 to Figure 14 are the concentration graphs over time for 20, 30 and 40 % displayed. The timescale is starting at 30 s. As described in

the previous section, this is due to the flushing sequence beforehand.

For all three concentrations a deviation in concentrations between the temperatures is noticeable, especially at 70 °C. Since the system is a closed loop, no mass was lost and the batches were the same for the tests. A possible explanation is that the tests from 30 to 70 °C were conducted consecutively. It is possible that the temperature input was locally above the decomposition point of urea (133 °C). Therefore, some urea decomposed. Furthermore, this process is enhanced through the continuous withdrawal of UWS from the system. When emptying, the heating coil is just partially covered in UWS, promoting potential decomposition as well. This would explain why the concentration is decreasing from 30 to 70 °C for the same batch.

Regarding the concentration itself, it is noticeable that the concentration is increasing strongly until 40 s. Afterwards the gradient smoothens towards linear behaviour and increases constantly.

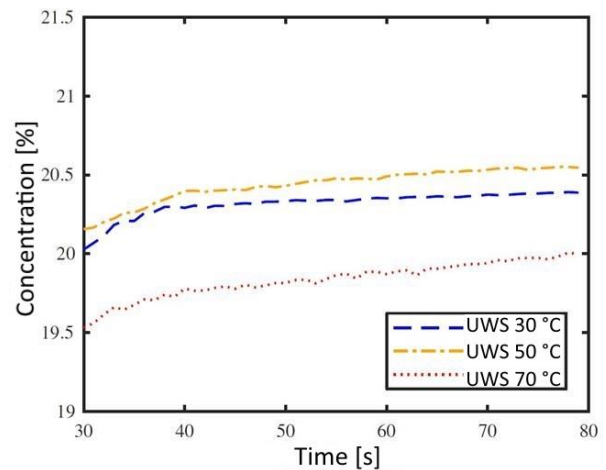


Figure 12. Change in concentration for 20 % UWS.

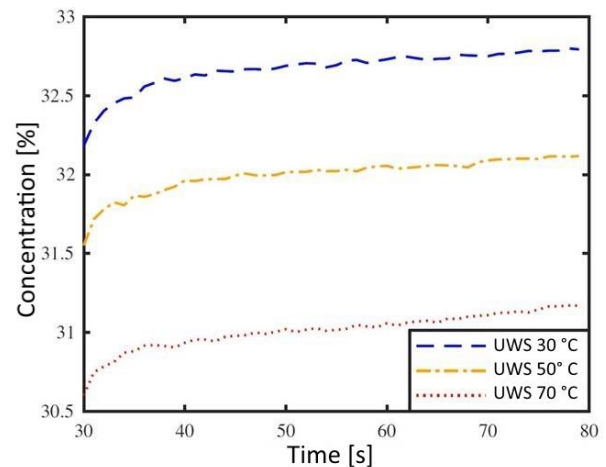


Figure 13. Change in concentration for 30 % UWS.

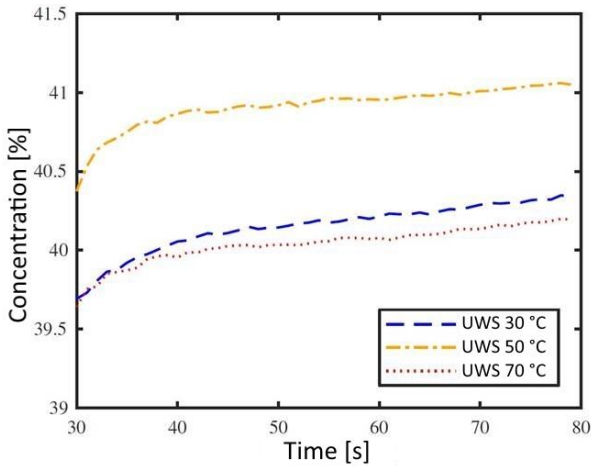


Figure 14. Change in concentration for 40 % UWS.

The change in gradients is due to the test setup and sequence. Whilst the linear gradient starting at 40 s is salt segregation and accumulation due to cavitation, the first gradient is of different nature. In Figure 15 the concentration for a 40 % UWS at 70 °C is displayed starting at 27 s. At 28.5 s a decline in concentration is detected before the concentration increases steeply until 38 s and going into the linear behaviour. One possible reason for this behaviour is the temperature influence. When flushing with cold water just before the test with UWS starts, the connector pipes and solenoid valve cool down ( $T_{MV}$ ). This is depicted in Figure 16. These two parts are used mutually for water and UWS. The temperature of the solenoid valve is cooled down to 67.9 °C at 20 s. After the valve opened the injection temperature ( $T_{inj}$ ) of UWS dropped to 64.9 °C before it recovered to 69.4 °C at 34 s. Due to the temperature decrease, the refractive index increases which is detected as a decrease in concentration. However, it is a temperature effect by nature. At 40 s the temperature has recovered and is constant. The following linear increase is solely a change in concentration.

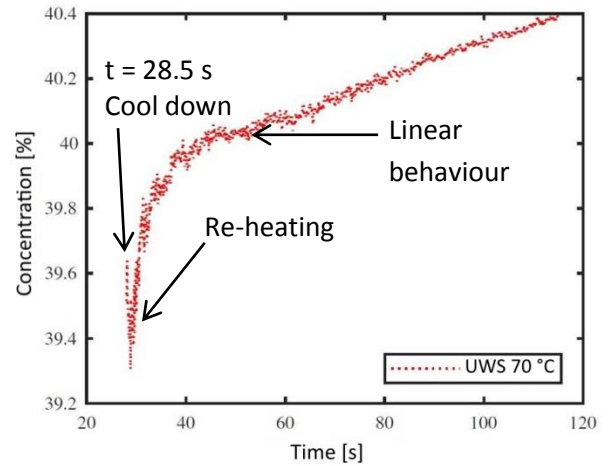


Figure 15. Change in concentration for a injection time of 90 s with 40 % UWS at 70 °C.

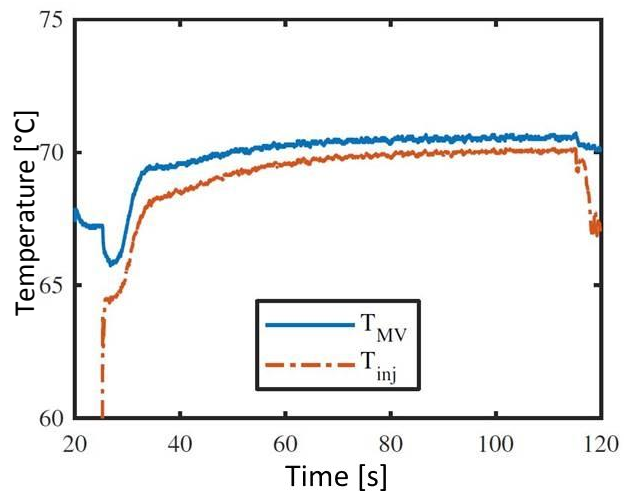


Figure 16. Temperature curves for solenoid valve ( $T_{MV}$ ) and injection temperature ( $T_{inj}$ ).

The influence of concentration of the UWS on the degree of segregation is depicted in Figure 17. Since the influence of temperature seems to be negligible, the change in concentration ( $\Delta c$ ) was averaged for all three temperatures. Thereby, the data used was between 40 s until the end of the test. Figure 17 shows a linear increase in degree of segregation with increasing UWS concentration. For 20 %  $\Delta c$  is 0.157 % rising to 0.193 % for 30 %, and to 0.233 % for 40 % UWS.

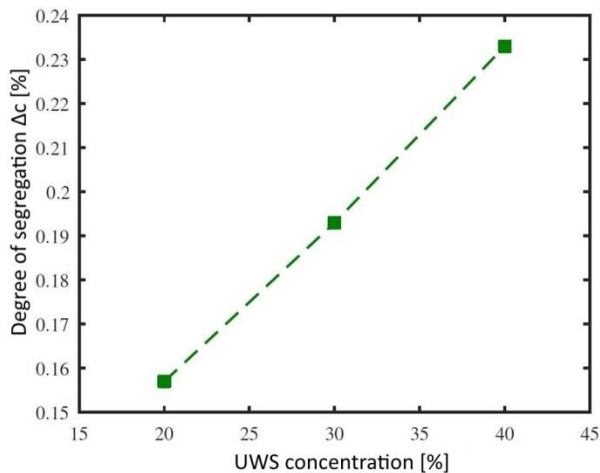


Figure 17. Influence of UWS concentration on degree of segregation.

## 5. SUMMARY & DISCUSSION

In this paper it was possible to proof a connection between occurring cavitation and the segregation of solved salt. Additionally, the salt accumulates upstream. In this case urea salt was used as ADN-simuli. The measurements were based on laser refraction. A prior calibration in terms of temperature and concentration is mandatory. In this case no significant temperature influence was detectable. It seems not to be strong enough and is superimposed by the change in concentration. However, for every temperature segregation and accumulation of salt could be shown. Furthermore, the degree of segregation seems to increase linearly with increasing salt concentration. Therefore, the risk of clogging of crucial parts is increased as well. Especially for highly concentrated ADN-based monopropellants like LPM-103S and FLP-106 with ADN-concentrations of 63 % and 64.9 % respectively.

## 6. OUTLOOK

The influence on salt segregation should be investigated further and be extended to more sophisticated propellant blends like LMP-103S. The parameters driving it need to be identified. This includes a possible temperature influence which could be investigated separately.

## 7. ACKNOWLEDGEMENTS

The authors would like to thank Lukas Werling, Ingo Dörr, Jan Buddenberg and Hagen Friedrich at DLR test bench M11 in Lampoldshausen for their support of the test campaign.

## 8. REFERENCES

- [1] Larsson A, Wingborg N. Green Propellants Based on Ammonium Dinitramide (ADN). In: Hall DJ, editor. *Adv. Spacecr. Technol.*, InTech; 2011. doi:10.5772/13640.
- [2] Persson M, Anflo K, Dinardi A. A Family of Thrusters for ADN-Based Monopropellant LMP-103S. 48th AIAAASMEASAEASEE Jt. Propuls. Conf. Exhib., American Institute of Aeronautics and Astronautics (AIAA); 2012. doi:10.2514/6.2012-3815.
- [3] Hendrich C, Schlechtriem S. Flashing Behavior of Ionic Liquid Propellants under Vacuum Conditions. 51st AIAASAEASEE Jt. Propuls. Conf., American Institute of Aeronautics and Astronautics (AIAA); 2015. doi:10.2514/6.2015-4124.
- [4] Hendrich C, Gury L, Schlechtriem S. Predicting Flashing Phenomena: A Combined Approach of Numerical Simulation and Experiments. 52nd AIAASAEASEE Jt. Propuls. Conf., American Institute of Aeronautics and Astronautics (AIAA); 2016. doi:10.2514/6.2016-4663.
- [5] Friedhoff P, Hawkins A, Carrico J, Dyer J, Anflo K. On-Orbit Operation and Performance of Ammonium Dinitramide (ADN) Based High Performance Green Propulsion (HPGP) Systems. 53rd AIAASAEASEE Jt. Propuls. Conf., American Institute of Aeronautics and Astronautics; 2017. doi:10.2514/6.2017-4673.
- [6] Dinardi A, Anflo K, Friedhoff P. On-Orbit Commissioning of High Performance Green Propulsion (HPGP) in the SkySat Constellation 2017.
- [7] Peter EM, Takimoto A, Hayashi Y. Flashing and Shattering Phenomena of Superheated Liquid Jets. *JSME Int J* 1994;37:313–21.
- [8] Bashkatov AN, Genina EA. Water refractive index in dependence on temperature and wavelength: a simple approximation. *Saratov Fall Meet. 2002 Opt. Technol. Biophys. Med.* IV, vol. 5068, International Society for Optics and Photonics; 2003, p. 393–396.
- [9] Venkatesan VK, Suryanarayana CV. Conductance and other physical properties of urea solutions. *J Phys Chem* 1956;60:775–776. doi:10.1021/j150540a016.